ASM Sc. J., 18, 2023

https://doi.org/10.32802/asmscj.2023.1295

The Impact of Sodium Perylene-3, 4, 9, 10-Tetracarboxylate Surfactant Concentration on the Yield of Liquid Phase Exfoliated Graphene Sheets

N. J. Ahmad[1], R. Mohamed[1,2*], M.F. Malek[1, 3], S.M. Sanusi[1], M.A. Muhamad[1] and M. Rusop[2,3]

[1]*Faculty of Applied Sciences, Universiti Teknologi MARA, 40450 Shah Alam, Selangor, Malaysia*

[2]*NANO-SciTech Lab (NST), Centre for Functional Materials and Nanotechnology (FMN), Institute of Science (IOS), Universiti Teknologi MARA, 40450 Shah Alam, Selangor, Malaysia*

[3]*NANO-ElecTronic Centre (NET), Faculty of Electrical Engineering, Universiti Teknologi MARA, 40450 Shah Alam, Selangor, Malaysia*

The graphene sheets were aqueous processed via simple method liquid phase exfoliation. Sodium perylene-3, 4, 9, 10-tetracarboxylate (NaPTCA) were used as surfactant to assist the exfoliation process. The purpose of this research is to investigate the impact of NaPTCA concentration on the yield of liquid phase exfoliation of graphite to graphene sheets. The degree of exfoliation was found to be greatly influenced upon the concentration of NaPTCA surfactant. 1.0 mgm L^{-1} was identified as the optimal NaPTCA concentration as the graphene produced had a distinct x-ray diffraction crystallinity, scanning electron microscopic image features, high concentration of graphene dispersion (0.154 mgmL^{-1}) and high conductivity values (751.88 Sm^{-1}) in 2-probe electrical measurements, all of which comparison are much favourably with typical values obtained for multi-layer graphene. Hence, this simple approach for liquid-phase graphite exfoliation provides decent potential for mass production of high-quality graphene for a wide range of applications in energy storage, optical, and electronic areas.

Keywords: Graphene; liquid phase exfoliation; hydrothermal; surfactant; concentration

I. INTRODUCTION

Graphene is a novel form of two-dimensional (2D) carbon nanomaterial that originates as a single layer of densely packed carbon atoms in a honeycomb lattice (Dhand *et. al.*, 2020; Gu *et al.*, 2019). It is the fundamental building block for all other dimensions of graphitic materials (Salifairus *et al.*, 2016). Graphene has a broad range of applications like, high speed transistors, transparent/flexible electrodes and films (Ricciardulli *et. al.*, 2018; N. Zhang *et al.*, 2019), sensors (Farmani & Mir, 2019; Zheng & Wang, 2019), energy storage (Ma *et al.*, 2020), alkali metal ions battery (Y. Zhang *et. al.*, 2019; Liu *et al.*, 2017) and, composites (Alimoradi, 2018) which these were achievable owing to its distinctive mechanical (Huang *et. al.*, 2015; Zhao *et al.*, 2010), electrical (Vasanthi *et. al.*, 2020; Haditale, Dariani & Ghasemian Lemraski, 2019), and thermal characteristics (Yassin *et al.*, 2019). One of the significant obstacles in certain essential types of applications, such as printed electronics, and conductive coatings is that the unavailability of industrial-scale techniques for synthesising high-quality graphene in the form of liquid inks, and dispersions. Coleman *et al.* first discovered liquid phase exfoliation (LPE) of graphite powder using sonication of graphite suspensions in 2008, achieving few layer graphene production and heralding the birth of the LPE process (Coleman *et al.*, 2008). This LPE, a new top-down approach, could yield a stable dispersion of monolayer or few-layer defect-free graphene by simply exfoliating

*Corresponding author's e-mail: ruzianamohd@uitm.edu.my

natural graphite with high-shear mixing or sonication (Ciesielski & Samorì, 2014). Since one of the graphene traits is hydrophobic (Li *et al.*, 2008), the stabilisation of the dispersion may become the major problem. LPE facilitates the stabilisation of the graphene dispersions either thermodynamically via suitable solvents or electrostatically via surfactants (Griffin *et al.*, 2020). Surfactant exfoliation, in particular, is appealing since all processing takes place in aqueous conditions.

Perylene-3, 4, 9, 10-tetracarboxylate (PTCA) is a novel exfoliator for graphene in aqueous condition. PTCA is a liquid-soluble type of π-conjugated n-type organic semiconductor compound PTCDA (perylene tetracarboxylic acid dianhydride) (Wang *et al.*, 2013). PTCA is able to noncovalently attach to the graphene surface through π-π stacking to induce exfoliation of graphite in water (Wang *et al.*, 2013). In terms of stabilisation, the tetra-anionic state of the PTCA provides the required inter-flake repulsive electrostatic forces for stable dispersions (Wang *et al.*, 2013). Narayan *et al.* obtained a stable dispersion of graphene in PTCA up to 200 μgmL^{-1} after 3 h bath sonication followed by centrifugation. Unfortunately, low sonication time yielding low concentration of graphene dispersion. Exposure to long sonication duration may increase the graphene yield i.e., 0.5 $mgmL^{-1}$ after 12 hours of sonication in the aqueous solvent (Narayan *et al.*, 2017). Consequently, the flake size will reduce considerably and the number of defects in the graphene will also continuously increase during this procedure. In attempt to overcome the use of long sonication process in LPE method, various auxiliary compounds were implemented such as magnetic nanoparticle Fe_3O_4 as "particle wedges (Yang *et al.*, 2020) and naphthalene (Xu *et al.*, 2014), intercalation of salt in organic solvent (Li *et. al.*, 2019; Wang, Wang & Ji, 2017) and alkali metal ions (Cheng, Kong & Liu, 2019; Seidl *et al.*, 2017). Among them, intercalation with alkali metal ion exhibits great outcome alongside the simplicity in combining with other solvents.

In this paper, the current PTCA surfactant was customised by adding the alkali metal ions of sodium for the synthesisation of high-yield few-layer graphene. Large ionic radius of sodium able to facilitate the exfoliation process by conquering the energy barrier allowing the intercalation to occur. The effects of NaPTCA surfactant concentration was methodically investigated. A series of characterisations depicts that the efficiency of the exfoliation process was highly influenced from the concentration of NaPTCA surfactant.

II. MATERIALS AND METHOD

A. Materials

The pristine graphite flakes (325 mesh, 43209) was acquired from Alfa Aesar. Perylene-3,4,9,10-tetracarboxylic dianhydride (PTCDA), potassium hydroxide (KOH), and sodium carbonate (Na_2CO_3) were acquired from Sigma Aldrich and ethanol (95% purity) used without additional purification. All solutions were prepared using deionised water, as were the samples' washing and dialysis.

B. Preparation of NaPTCA Surfactant

PTCDA must be converted or reduced to PTCA before the Na-PTCA surfactants can be prepared. PTCDA was commonly reduced to PTCA by dissolving 0.715 g of KOH pellets in 500 ml water and then adding 1 g of red PTCDA powder. The mixture was heated for 1 hour at 80 °C until it produced a green homogeneous solution. After filtering the residue, 1 M HCl was progressively added until a very immiscible brick-red precipitate formed. The mixture was then agitated for 1 hour at room temperature. The mixture was dried overnight in a vacuum oven. PTCA was identified as a reddish solid orange.

NaPTCA was made by mixing 2.50 g of PTCA and 1.0 g of Sodium Carbonate (Na_2CO_3) in 100 ml of ethanol and deionised water in a 1:1 (v/v) ratio. The mixture was stirred for three days at 60 °C before being centrifuged for 30 minutes at 5000 rpm. The precipitation was then collected and dried overnight at 150 °C. NaPTCA is identified as the yellow powder.

C. Preparation of Hydrothermal Liquid Phase Exfoliation (LPE) Graphene

In a typical preparation, 5 mg of NaPTCA powder was dissolved in 50 mL deionised water and stirred for 1 h to get a complete suspension of 0.1 $mgmL^{-1}$ NaPTCA surfactant concentration. The graphite flakes were added to the aqueous 0.1 $mgmL^{-1}$ NaPTCA surfactant to make a final graphite

concentration of 0.25 mgmL^{-1}. The mixture of the graphite and the NaPTCA surfactant was treated under hydrothermal conditions for 15 hours. Then, the pre-treated mixture was sonicated in a bath sonicator for 2 h. The sonication created black suspensions, which were allowed to stand overnight before being centrifuged at 5000 rpm for 30 minutes to eliminate unexfoliated graphitic particles. The supernatant of the centrifugation tube resembles as the graphene dispersion. The process of graphene formation was repeated with various NaPTCA surfactant concentrations with other concentration ranging from 0.5 mgmL^{-1} – 2.0 mgmL^{-1}.

D. Characterisation

A X'Pert PRO MPD diffractometer (PANalytical, UK) was used to measure the X-ray diffraction of graphite and exfoliated materials. The information of the diffracted angle is used to determine the d-spacing which correlated to the exfoliation efficacy. Scanning electron microscopy (SEM, Vega 3, Tescan Analytics, UK) was used to image the morphology of graphene sheets. Two probe systems were used to test the conductivity of the exfoliated samples. Surface profiler (P – 6, KLA – Tencor, US) was used to measure the thickness of the samples. A UV-Visible spectrometer (Cary 5000, Varians, US) was used to examine the sample's optical characteristics.

III. RESULTS AND DISCUSSION

A. Scanning Electron Microscope (SEM)

SEM was used to analyse the structures and morphologies of the exfoliated graphene sheets. The SEM images of pure graphite powder and exfoliated graphene sheets in varied NaPTCA surfactant concentrations are shown in Figure 1. The pure graphite powders were mainly composed of asymmetrical flakes with a vast range of thicknesses and average lateral diameters of 46.22 µm, as illustrated in Figure 1. Exfoliation began immediately after the addition of NaPTCA, when a small segment of graphite was seen to be detached from the bulk graphite and clearly shaped into a flake-like structure. It was discovered that when NaPTCA concentration increased, the lateral size of the exfoliated graphene sheets decreased until it reached an eigenvalue of 1.0 mgmL^{-1}, where the lateral size of the exfoliated graphene sheets was the smallest 3.69 µm. Furthermore, the exfoliated graphene flakes sampled in 1.0 mgmL^{-1} appear to be smaller and more uniform compared to other samples. We also discovered that the exfoliated graphene sample in 1.0 mgmL^{-1} NaPTCA was randomly oriented with a thin layer and is strongly bonded like compact bedded rock.

Table 1. The lateral size of graphene in various NaPTCA surfactant concentrations

Sample of NaPTCA surfactant at various concentration (mgmL^{-1})	**Lateral size (µm)**
0.1	8.89
0.5	7.93
1.0	3.69
1.5	6.17
2.0	11.62

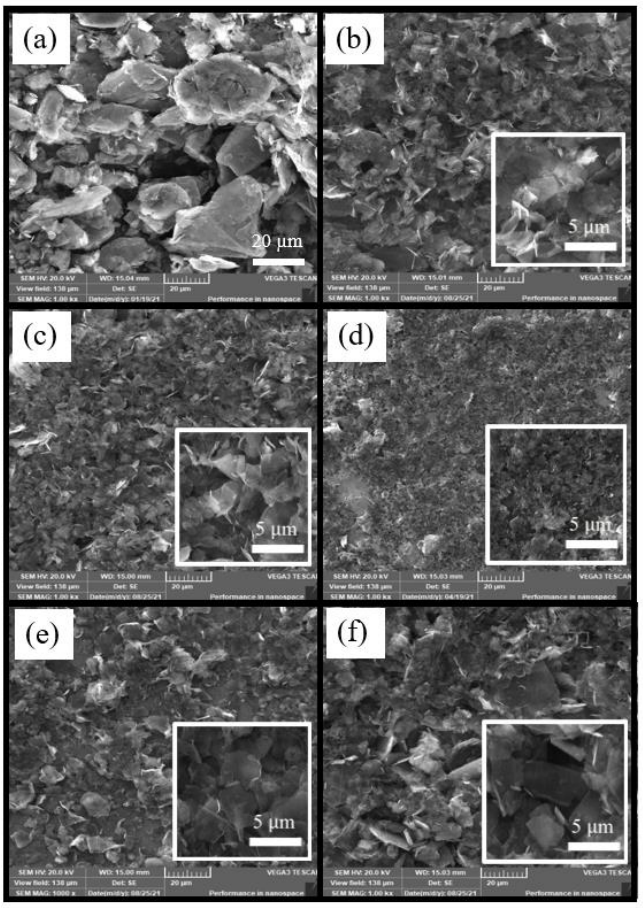

Figure 1. SEM images of (a) graphite and graphite sample with NaPTCA surfactant at concentration, (b) 0.1 mgmL^{-1}, (c) 0.5 mgmL^{-1}, (d) 1.0 mgmL^{-1}, (e) 1.5 mgmL^{-1}, and (f) 2.0 mgmL^{-1}

Furthermore, as observed in the inset (magnification 5000x) in Figure 1 (d), the samples show evenly scattered and separated flakes. This indicates that 1.0 mgmL^{-1} NaPTCA is the optimal concentration for effective exfoliation.

This clarify that suitable surfactant concentration will aid the graphene exfoliation process as the use of surfactant able to reduce the surface energy of graphene (46.7 mJm^{-2}) allowing the graphene exfoliation to occur at ease (Vacacela Gomez *et al.*, 2021). It is suggested that the surface energy of 1.0 mgmL^{-1} of NaPTCA surfactant may close to 46.7 mJm^{-2} causing the graphene sample with this surfactant concentration to greatly exfoliated and have the smallest lateral dimension. At high concentrations of NaPTCA, however, we discovered that the exfoliation process is massively reduced and began to accumulate as the lateral size of the sample on 1.5 mgmL^{-1} and 2.0 mgmL^{-1} NaPTCA rose back to 6.17 µm and 11.62 µm, respectively.

B. Energy Dispersive X-Ray Spectroscopy (EDX)

The quantitative EDX spectrum (Figure 2) demonstrated the presence of C, O and Na peak at corresponding 0.15 keV, 0.25 keV and 1.0 keV.

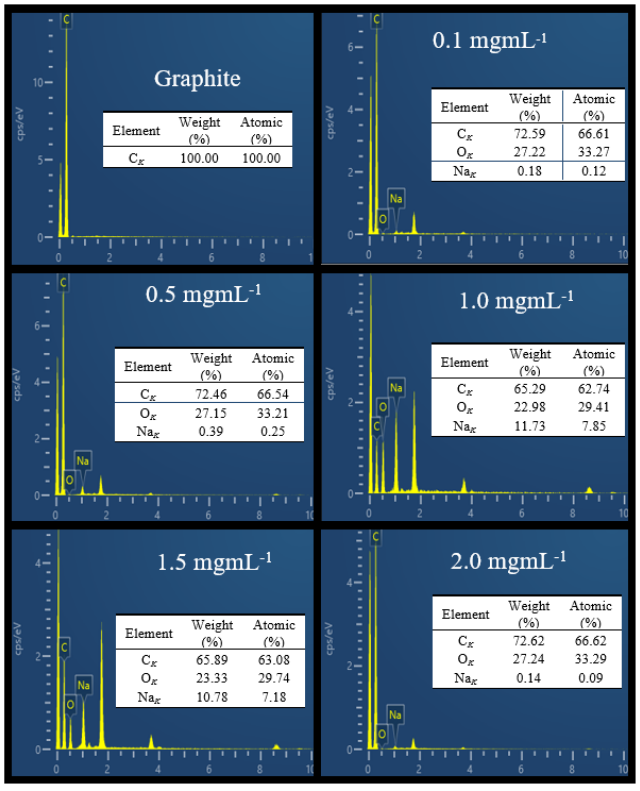

Figure 2. EDX spectrum of graphite with various concentrations of NaPTCA surfactant

High atomic intensity of C was observed at pure graphite. This is corresponding to the graphitic structure that mainly composed of carbon atoms (Siburian *et al.*, 2018). The intensity of Na was the highest at 1.0 mgmL^{-1} followed with lowest C peak intensity. This indicates that the more Na atom was successfully intercalated the graphite and ease the exfoliation process. This can be seen from the reduction of C peak intensity as an indication of the presence of graphene. This reduction occurs due to the low bonding in between the C atoms as most of the graphite layer were exfoliated to graphene. This further explains the decreased in the lateral size for sample at 1.0 mgmL^{-1}.

C. X-Ray Diffraction Analysis (XRD)

Figure 3 displays the evaluation of pure graphite structure with a distinct and strong basal diffraction peak of (002) plane at 26.49° demonstrating high crystallinity of graphitic materials (Saiful Badri *et al.*, 2017). It has been well established that the peak intensity was in relation to the number of layer of the graphene sheets (Hadi *et al.*, 2018).

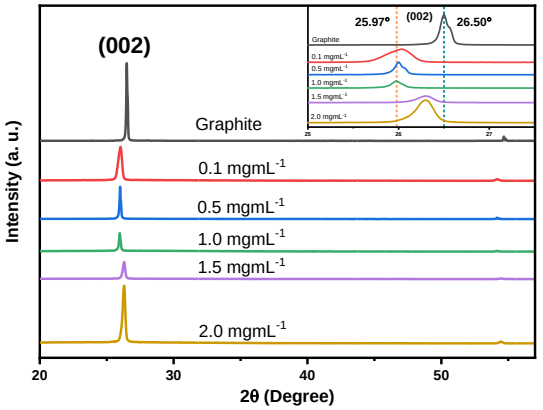

Figure 3. XRD patterns of graphite with various concentrations of NaPTCA surfactant.

The peak intensity at the (002) plane was mildly attenuated and broadened with the addition of NaPTCA surfactant at 0.1 mgmL^{-1}, then dramatically declined at 1.0 mgmL^{-1} and progressively rose again. The reduction of the peak intensity happens as a result of the decreasing in the thicknesses indicating the exfoliation process was carried out efficiently during the sonication process (Saiful Badri *et al.*, 2017). The relative peak intensity of each sample was computed to estimate the relative value since the peak intensity at 1.0

mgmL^{-1} and 1.5 mgmL^{-1} samples were found to be almost identical. According to the computation, 1.0 mgmL^{-1} has the lowest relative intensity value (0.077) compared to 1.5 mgmL^{-1} (0.083), indicating that the exfoliated graphene sample at 1.0 mgmL^{-1} has the thinnest layer. Interestingly, the diffraction angle of graphite samples at various NaPTCA concentrations was shown to be somewhat shifted to a lower angle ($2\theta = 25.97°$). This decrease in diffraction angle was primarily caused by an increase in the d-spacing between the graphene interlayers (Wang *et al.*, 2017). The d-spacing of each sample was computed using Bragg's equation, which is given below:

$$2d\ sin\ \theta\ = n\lambda \quad (1)$$

According to Table 2, the sample at 1.0 mgmL^{-1} of NaPTCA surfactant had the largest d-spacing 0.344 nm compared to graphite 0.336 nm. The increment of the d-spacing indicating the exfoliation of graphite to form graphene was a success as the van der Waals forces that held the graphene layer were effectively demolished (Wang, Wang & Ji, 2017). This reveals that 1.0 mgmL^{-1} of NaPTCA surfactant was the optimal concentration to synthesise graphene.

Table 2. d-spacing and relative peak intensity at (002) for graphite and graphite with various concentrations of NaPTCA surfactant

Sample of Graphite and NaPTCA surfactant at various concentration	d-spacing (nm)	Relative Peak Intensity at (002)
Graphite	0.336	0.323
0.1 mgmL^{-1}	0.342	0.145
0.5 mgmL^{-1}	0.342	0.135
1.0 mgmL^{-1}	0.344	0.077
1.5 mgmL^{-1}	0.335	0.083
2.0 mgmL^{-1}	0.335	0.238

C. Fourier Transform Infrared Spectroscopy (FTIR)

Figure 4 illustrates the wide scan FTIR spectra of graphite with NaPTCA surfactant with varying concentration.

Table 3. Peak assignments of the FTIR spectrum of graphite sample with various NaPTCA surfactant concentrations

No.	Frequency wavenumber (cm^{-1})						Assignment	References
	Graphite	0.1 mgmL^{-1}	0.5 mgmL^{-1}	1.0 mgmL^{-1}	1.5 mgmL^{-1}	2.0 mgmL^{-1}		
1.	-	-	-	3313.00	-	-	O – H stretching bond of hydroxyl group	(Yang *et. al.*, 2020; Teng *et. al.*, 2019; Manna *et. al.*, 2016; Xu *et al.*, 2014)
2.	2232.30	2327.33	2316.30	2309.40	2285.94	2304.57	N = C = S stretching vibration	(Iqbal *et. al.*, 2021; Nandiyanto, Oktiani & Ragadhita, 2019)
3.	2113.40	2076.26	2111.43	-	2069.36	2076.26		
4.	-	1535.48	1514.79	1535.48	1535.48	-	C = O vibration of carboxyl group	(Yang *et. al.*, 2020; Cheng, Kong & Liu, 2019; Wang *et al.*, 2013)
5.	-	-	-	1387.87	-	-	Aromatic C = C stretching vibration	(Sukumaran *et. al.*, 2019; Xu *et. al.*, 2014; Wang *et al.*, 2013)
6.	974.77	972.64	972.64	972.64	972.64	972.64	Aromatic C – H in-plane bend	(Nandiyanto, Oktiani & Ragadhita, 2019; Sayah *et al.*, 2018)
7.	-	874.00	878.14	855.00	855.00	871.24	Aromatic C – H out-of-plane bend	(Nandiyanto, Oktiani & Ragadhita, 2019; Sayah *et al.*, 2018)

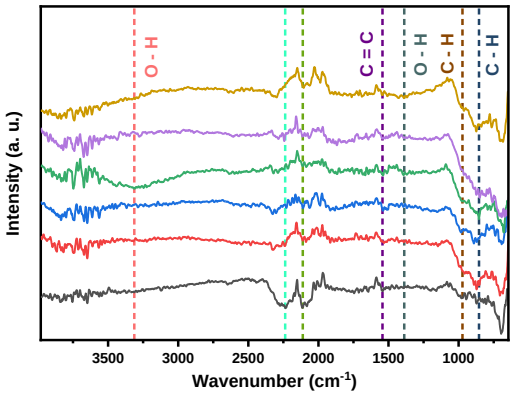

Figure 4. FTIR spectrum of graphite with various concentrations of NaPTCA surfactant

Two major peaks appear at 2113.40 cm^{-1} and 2232.30 cm^{-1} for pure graphite which corresponds to typical inorganic ions such as isothiocyanate ions (Nandiyanto, Oktiani & Ragadhita, 2019; Iqbal *et al.*, 2021). Common pattern of graphene materials was observed at peak 1535.48 cm^{-1}, which attributed to C = C bond, comes from the sp^2 carbon atoms in honeycomb lattices of graphene (Sayyad, Balakrishnan & Ajayan, 2011; Hadi *et al.*, 2018). All samples show a peak at 972.64 cm^{-1}, which is caused by the aromatic C – H in-plane bend (Nandiyanto, Oktiani & Ragadhita, 2019; Sayah *et al.*, 2018). Peak values of 855.00 – 878.14 cm^{-1} were observed for all samples after the addition of NaPTCA surfactant. This peak is correlated to the C – H out-of-plane bend (Nandiyanto, Oktiani & Ragadhita, 2019; Sayah *et al.*, 2018). Peaks at 972.64 cm^{-1} can be found in all samples. This demonstrates that the NaPTCA surfactant was successful in intercalating the graphite interlayer and driving some carbon atoms out of plane (Wang, Wang & Ji, 2017). Furthermore, only the sample containing 1.0 $mgmL^{-1}$ of NaPTCA showed two peaks at 1387.87 cm^{-1} and 3313.00 cm^{-1}. The initial peak, 1387.87 cm-1, was associated with –OH vibrations and energy of the single bond between C and O stretching of C – O – C and C – OH, reflecting an increase in oxygen content following effective exfoliation (Cheng, Kong & Liu, 2019). Whereas the second peak of 3313.00 cm^{-1} is referring to the stretching vibrations of the –OH bond indicating the presence of hydroxyl groups (Yang *et al.*, 2020). Hence, 1.0 mg/ml of NaPTCA surfactant is suitable to synthesise graphene as graphene was successfully exfoliated with minimal defects in the following concentration.

D. Ultraviolet-Visible Analysis (UV-Vis)

The impact of NaPTCA concentration on the degree of graphene exfoliation from graphite was studied using UV-Vis spectroscopy.

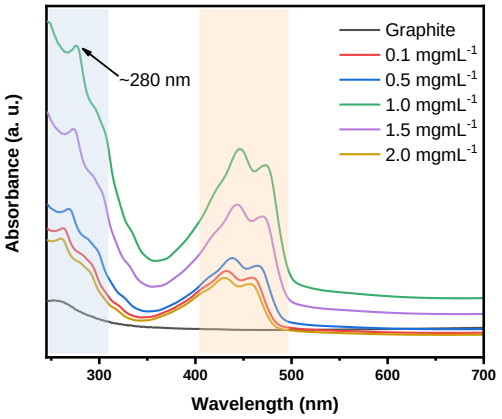

Figure 5. UV-Vis absorbance peak intensity of graphite with various concentrations of NaPTCA surfactant

Figure 5 shows that the absorbance of the graphite sample at approximately 250 nm. Graphene is distinguished by a peak centred at around 260 nm to 300 nm (Durge, Kshirsagar & Tambe, 2014). This can be seen after the addition of NaPTCA surfactant where the absorbance peak was slightly shifted to a higher wavelength 260 nm and reaches to maximum at 280 nm at 1.0 $mgmL^{-1}$. The wavelength ranges from 260 nm to 280 nm was attributed to the n – π^* of the carbonyl (C = O) group (Uran, Alhani & Silva, 2017; Emiru & Ayele, 2017) Wavelength shifted to a higher value is known as the redshifted phenomenon (Li *et al.*, 2008). The occurrence of this redshift phenomenon shows that changes in electronic conjugation happened as a result of structural ordering after the removal of the sp^3 carbon atom to generate the sp^2 carbon atom (Krishnamoorthy *et al.*, 2012) The replacement of sp^2 carbon atoms upon graphene exfoliation from graphite results in an increase in electron concentration because more delocalised electrons were present (Emiru & Ayele, 2017) Moreover, the concentration or the quantity of the graphene produced can be estimated from the value of the absorbance. Lambert-Beer's law was utilised to calculate the concentration of graphene dispersed.

$$A = \alpha \cdot C \cdot l \quad (2)$$

Where α is the absorption coefficient (1390 $mgmL^{-1}m^{-1}$) for graphene diffuse in surfactant solution (Gomez *et. al.*, 2019; Lotya *et al.*, 2009), C is the dispersed graphene solution concentration, and l is the optical path length (10 mm). As per the calculations, the maximum graphene dispersion (0.154 $mgml^{-1}$) was achieved at 1.0 $mgmL^{-1}$ NaPTCA surfactant. This explains the increase in delocalised electrons which arising from the exfoliated graphene sheets.

Table 4. The concentration of graphene dispersions with various concentration of NaPTCA surfactant.and overall production yield

Sample of NaPTCA surfactant at various concentration	Concentration of graphene dispersion, C ($mgmL^{-1}$)	Graphene production yield (wt%)
0.1 $mgmL^{-1}$	0.064	25.6
0.5 $mgmL^{-1}$	0.074	29.6
1.0 $mgmL^{-1}$	0.154	61.6
1.5 $mgmL^{-1}$	0.113	45.2
2.0 $mgmL^{-1}$	0.059	23.6

Finally, using Equation (3), the graphene yield is estimated.

$$Y\ (wt\%) = \left(\frac{C}{C_o}\right) \times 100 \qquad (3)$$

Where Y is the graphene yield in weight percent, C is the final concentration of graphene dispersion, and C_o is the initial graphite concentration (0.3 $mgmL^{-1}$). As tabulated from Table 4, 1.0 $mgmL^{-1}$ of NaPTCA surfactant is capable of exfoliating graphene up to 60% from the pristine graphite. As a result, 1.0 $mgmL^{-1}$ NaPTCA surfactant is the ideal concentration for exfoliating graphene sheets under aqueous conditions. The enormity of the surfactant may impede the exfoliation process and degrade graphene's unique features in every manner.

E. Current-Voltage Measurement (I-V)

To acquire a better knowledge of graphene electrical properties, current-voltage (I-V) characteristics were calculated and analysed for samples containing different concentrations of NaPTCA surfactant using a two-point probe device. The resistivity was computed using Equation (4) shown below:

$$\rho = \left(\frac{V}{I}\right) \cdot \frac{w \cdot t}{l} \qquad (4)$$

Where V denotes the applied voltage, I denotes the measured current, t denotes the thickness of the film as determined by a surface profiler, w denotes the electrode width (3.000 mm), and l denotes the distance between the electrodes (0.976 mm). The computed resistivity value is the reciprocal of the conductivity value.

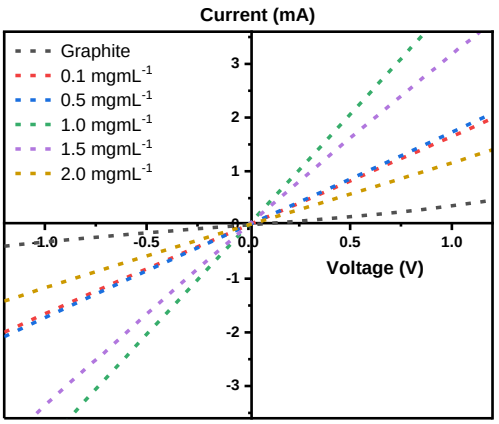

Figure 6. I-V characteristics of graphite with various concentrations of NaPTCA surfactant

Table 5. Resistivity and conductivity of graphite with various concentrations of NaPTCA surfactant

Sample of Graphite and NaPTCA surfactant at various concentration	Resistivity, ρ (Ω m)	Conductivity, σ (Sm^{-1})
Graphite	2.75×10^{-2}	36.36
0.1 $mgmL^{-1}$	1.13×10^{-2}	88.50
0.5 $mgmL^{-1}$	5.86×10^{-3}	170.65
1.0 $mgmL^{-1}$	1.33×10^{-3}	751.88
1.5 $mgmL^{-1}$	1.56×10^{-3}	641.03
2.0 $mgmL^{-1}$	1.41×10^{-2}	70.92

From Table 4, the highest conductivity value was observed for sample with 1.0 $mgmL^{-1}$ NaPTCA surfactant (751.88 Sm^{-1}). This result is comparable to that in UV-Vis, which is in relation to the large amount of carrier concentration. Furthermore, the increment of carrier concentration is an indication of successful exfoliation as the graphene was exfoliated, the layer was separated and the π electrons that were loosely attached are not densely included

in the layer binding leading to greater electron mobility (Aparna *et al.*, 2013).

Table 6. Comparison of conductivity of graphene with other research studies

No.	Method	Conductivity, σ (Sm^{-1})	Reference
1.	Ozone treatment	1400	(Rider *et al.*, 2014)
2.	Electrochemical exfoliation / BMIM-DBS	2.71×10^{-7}	(Mohamed *et al.*, 2018)
3.	Chemical Vapor Deposition	768	(Zhang *et al.*, 2014)
4.	Liquid-phase exfoliation sonication / Water	100	(Hernandez *et al.*, 2008)
5.	Liquid-phase exfoliation sonication / DMF	744	(Vasanthi *et al.*, 2020)
6.	Hydrothermal	704	(Garcia-Bordejé, Benito & Maser, 2021)
7.	Liquid-phase exfoliation hydrothermal / NaPTCA	752	This work

Graphene can be obtained in various method. Each method gives different outcome. The greater the complexity of the method, the better the conductivity of the graphene obtained. As observed, the ozone treatment method able to achieve graphene with highest conductivity of 1400 Sm^{-1} Followed by chemical vapor deposition method, this method is one of the most favourable methods to achieve finest graphene with relevant conductivity. Graphene obtained via CVD method achieve up to 768 Sm^{-1}. Due to the high cost and difficulties of this method, researcher find new method that could match up with the CVD which is called the liquid-phase exfoliation method. LPE is a facile, cost-effective and flexible method. Since it uses aqueous medium to exfoliate graphene, various solvent and surfactant can be studied in order to create ideal condition in producing large scale graphene with minimal defects. The electrical conductivity of graphene produced from only of LPE method was 100 Sm^{-1}. With the addition of DMF surfactant, the electrical conductivity of the exfoliated graphene was improved up to 744 Sm^{-1}. The increase of the electrical conductivity is the indication of high graphene concentration (Aparna *et al.,* 2013). For this work we use NaPTCA as the surfactant and the outcome is outstanding as the electrical conductivity was rose up to 752 Sm^{-1}. This suggest that our NaPTCA surfactant are the excellent exfoliant for graphene especially in aqueous medium condition.

IV. CONCLUSION

In this study, few-layers graphene was successfully synthesised from exfoliation of graphene sheets via sonication approach with the aid of NaPTCA conductive surfactant at various concentrations. SEM micrographs illustrate small particles of graphene flakes in 1.0 $mgmL^{-1}$ NaPTCA surfactant with the smallest lateral size to 3.69 μm. From XRD relative peak intensity at (002) plane, the as-exfoliated graphene in 1.0 $mgmL^{-1}$ of NaPTCA was the lowest (0.077) with highest interlayer d-spacing (0.344 nm). UV-Vis spectroscopic analysis verified the formation and the concentration of graphene were the highest in 1.0 $mgmL^{-1}$ NaPTCA surfactant (0.154 $mgmL^{-1}$) and up to ~62% of graphene were exfoliated from bulk graphite. This shows that NaPTCA at 1.0 $mgmL^{-1}$ is an excellent exfoliator as it able to offer ideal condition for graphene exfoliation leading to more graphene produced. The electrical properties of the graphene yield in 1.0 $mgmL^{-1}$ NaPTCA surfactant was notably increased with conductivity value up to 751.88 Scm^{-1}. This good electrical conductivity is a strong indicator of high amount of graphene is presence as more graphene layer produced, more free π electrons is presence. This explained on the great difference of electrical conductivity of graphene and graphite as in graphite most of the electrons were involved in the binding between the layer causing low existence of free electrons which then contributing to a much lower electrical conductivity. SEM, XRD, UV-Vis and IV analysis revealed that 1.0 $mgmL^{-1}$ NaPTCA surfactant is the optimum concentration to be used in facilitating the graphene synthetisation.

V. ACKNOWLEDGEMENT

This work was financially supported by the FRGS grants (IRMI/FRGS/5/3(264/2019)). We would like to convey our

special gratitude to the Faculty of Applied Sciences and NANO-SciTech Centre of Universiti Teknologi MARA (UiTM) Malaysia for their support in the process of characterisation. The first author would like to acknowledge the scholarship provided by the MyBrainSc program.

VI. CONFLICT OF INTEREST

The authors declare no conflict of interest.

VII. REFERENCES

Alimoradi, M 2018, 'Electro-exfoliation of graphite for large scale production of graphene and its composite with PANI for application in supercapacitors', J. Phys. Energy, vol. 2, pp. 0–31.

Aparna, R, Sivakumar, N, Balakrishnan, A, Sreekumar, NA, Shantikumar, NV & Subramanian, KRV 2013, 'An effective route to produce few-layer graphene using combinatorial ball milling and strong aqueous exfoliants', Journal of Renewable and Sustainable Energy, vol. 5, no. 3.

Binbin Z, Jinliang, S, Guanying, Y & Buxing, H 2014, 'Large-scale production of high-quality graphene using glucose and ferric chloride', Chemical Science, vol. 5, no. 12, pp. 4656–4660.

Cheng, ZL, Kong, YC & Liu, Z 2019, 'Li+/Na+ Co-Assisted Hydrothermal Exfoliation for Graphite into Few-Layer Graphene Nanosheets and Their Excellent Friction-Reducing Performance', ACS Sustainable Chemistry and Engineering, vol. 7, no. 24, pp. 19770–19778.

Ciesielski, A & Samorì, P 2014, 'Graphene via sonication assisted liquid-phase exfoliation', Chemical Society Reviews, vol. 43, no, 1, pp. 381–398.

Coleman, VA, Knut, R, Karis, O, Grennberg, H, Jansson, U, Quinlan, R, Holloway, BC, Sanyal, B & Eriksson, O 2008, 'Defect formation in graphene nanosheets by acid treatment: An x-ray absorption spectroscopy and density functional theory study', Journal of Physics D: Applied Physics, vol. 41, no. 6.

Dhand, V, Rhee, KY, Kim, HJ & Jung, DH 2020, 'A Comprehensive Review of Graphene Nanocomposites: Research Status and Trends', 2013.

Durge, R, Kshirsagar, RV & Tambe, P 2014, 'Effect of sonication energy on the yield of graphene nanosheets by liquid-phase exfoliation of graphite', Procedia Engineering, vol. 97, pp. 1457–1465.

Emiru, TF & Ayele, DW 2017, 'Controlled synthesis, characterization and reduction of graphene oxide: A convenient method for large scale production', Egyptian Journal of Basic and Applied Sciences, vol. 4, no. 1, pp. 74–79.

Farmani, A & Mir, A 2019, 'Graphene Sensor Based on Surface Plasmon Resonance for Optical Scanning', IEEE Photonics Technology Letters, vol. 31, no. 8, pp. 643–646.

Garcia-Bordejé, E, Benito, AM & Maser, WK 2021, 'Graphene aerogels via hydrothermal gelation of graphene oxide colloids: Fine-tuning of its porous and chemical properties and catalytic applications', Advances in Colloid and Interface Science, 292.

Gomez, CV, Tene, T, Guevara, M, Usca, GT, Colcha, D, Brito, H, Molina, R, Belluci, S & Tavolaro, A 2019, 'Preparation of few-layer graphene dispersions from hydrothermally expanded graphite', Applied Sciences (Switzerland), vol. 9, no. 12.

Griffin, A, Nisi, K, Pepper, J, Harvey, A, Szydlowska, BM, Coleman, JN & Backes, C 2020, 'Effect of Surfactant Choice and Concentration on the Dimensions and Yield of Liquid-Phase-Exfoliated Nanosheets', Chemistry of Materials, vol. 32, no. 7, pp. 2852–2862.

Gu, X, Zhao, Y, Sun, K, Viera, ALZ, Jia, Z, Cui, C, Wang, Z, Walsh, A & Huang, S 2019, 'Method of ultrasound-assisted liquid-phase exfoliation to prepare graphene', Ultrasonics Sonochemistry, vol. 58(March), p. 104630.

Hadi, A, Zahirifar, J, Sabet, JK & Dastbaz, A 2018, 'Graphene nanosheets preparation using magnetic nanoparticle assisted liquid phase exfoliation of graphite: The coupled effect of ultrasound and wedging nanoparticles', Ultrasonics Sonochemistry, vol. 44, pp. 204–214.

Haditale, M, Dariani, RS & Ghasemian Lemraski, E 2019, 'Electrical behavior of graphene under temperature effect and survey of I–T curve', Journal of Theoretical and Applied Physics, vol. 13, no. 4, pp. 351–356.

Hernandez, Y, Nicolosi, V, Lotya, M, Blighe, FM, Sun, Z, De, S, McGoverin, IT, Holland, B, Byrne, M, Gun'ko, YK, Boland, JJ, Niraj, P, Duesberg G, Krishnamurthy, S, Goodhue, R, Hutchison, J, Scardaci, V, Ferrari, AC & Coleman, JN 2008,

'High-yield production of graphene by liquid-phase exfoliation of graphite', Nature Nanotechnology, vol. 3, pp. 563–568.

Huang, HD, Zhou, SY, Ren, PG, Ji, X & Li, ZM 2015, 'Improved mechanical and barrier properties of low-density polyethylene nanocomposite films by incorporating hydrophobic graphene oxide nanosheets', RSC Advances, vol. 5, no. 98, pp. 80739–80748.

Iqbal, S, Bokhari, TH, Latif, S, Imran, M, Javaid, A & Mitu, L 2021, 'Structural and Morphological Studies of V2O5/MWCNTs and ZrO2/MWCNTs Composites as Photocatalysts', Journal of Chemistry, 2021.

Krishnamoorthy, K, Veerapandian, M, Mohan, R & Kim, SJ 2012, 'Investigation of Raman and photoluminescence studies of reduced graphene oxide sheets', Applied Physics A: Materials Science and Processing, vol. 106, no. 3, pp. 501–506.

Li, D, Muller, MB, Gilje, S, Kaner, RB & Wallace, GG 2008, 'Processable aqueous dispersions of graphene nanosheets', Nature Nanotechnology, vol. 3, no. 2, pp. 101–105.

Li, J, Yan, H, Dang, D, We,i W & Meng, L 2019, 'Salt and water co-assisted exfoliation of graphite in organic solvent for efficient and large scale production of high-quality graphene', Journal of Colloid and Interface Science, vol. 535, pp. 92–99.

Liu, T, Kim, KC, Lee, B, Chen, Z, Noda, S, Jang, SS & Lee, S W 2017, 'Self-polymerized dopamine as an organic cathode for Li- and Na-ion batteries', Energy and Environmental Science, vol. 10, no. 1, pp. 205–215.

Lotya, M, Hernandez, Y, King, PJ, Smith, RJ, Nicolosi, V, Karlsson, LS, Blighe, FM, De, S, Wang, Z, McGovern, IT, Duesberg, GS & Coleman, JN 2009, 'Liquid Phase Production of Graphene by Exfoliation of Graphite in Surfactant/Water Solutions', vol. 11, pp. 3611–3620.

Ma, F, Wang, X, Hu, Z, Hou, L, Yang, Y, Li, Z, He, Y & Zhu, H 2020, 'Batteries and Energy Storage Organic molecular electrode with ultra- high rate capability for supercapacitor'.

Manna, K, Huang, HN, Li, WT, Ho, YH & Chiang, WH 2016, 'Toward Understanding the Efficient Exfoliation of Layered Materials by Water-Assisted Cosolvent Liquid-Phase Exfoliation', Chemistry of Materials, vol. 28, no. 21, pp. 7586–7593.

Mohamed, A, Ardyani, T, Bakar, AA, Sagisaka, M, Umetsu, Y, Hussin, MRM, Ahmad, MK, Mamat, MH, King, S, Czajka, A, Hill, C & Eastoes, J 2018, 'Preparation of conductive cellulose paper through electrochemical exfoliation of graphite: The role of anionic surfactant ionic liquids as exfoliating and stabilizing agents', Carbohydrate Polymers, vol. 201, pp. 48–59.

Nandiyanto, ABD, Oktiani, R & Ragadhita, R 2019, 'How to read and interpret ftir spectroscope of organic material', Indonesian Journal of Science and Technology, vol. 4, no. 1, pp. 97–118.

Narayan, R, Lim, J, Jeon, T, Li, DJ & Kim, SO 2017, 'Perylene tetracarboxylate surfactant assisted liquid phase exfoliation of graphite into graphene nanosheets with facile re-dispersibility in aqueous/organic polar solvents', Carbon, vol. 119, pp. 555–568.

Ricciardulli, AG, Yang, S, Wetzelaer, GJAH, Feng, X & Blom, PWM 2018, 'Hybrid Silver Nanowire and Graphene-Based Solution-Processed Transparent Electrode for Organic Optoelectronics', Advanced Functional Materials, vol. 28, no. 14, pp. 1–6.

Rider, AN, Thostenson, ET & Brack, N 2014, 'Ultrasonicated-ozone modification of exfoliated graphite for stable aqueous graphitic nanoplatelet dispersions', Nanotechnology, vol. 25, no. 49.

Saiful Badri, MA, Salleh, MM, Md Noor, NF, Rahman, MYA & Umar, AA 2017, 'Green synthesis of few-layered graphene from aqueous processed graphite exfoliation for graphene thin film preparation', Materials Chemistry and Physics, vol. 193, pp. 212–219.

Salifairus, MJ, Abd Hamid, SB, Soga, T, Alrokyan, SAH, Khan, HA & Rusop, M 2016, 'Structural and optical properties of graphene from green carbon source via thermal chemical vapor deposition', Journal of Materials Research, vol. 31, no. 13, pp. 1947–1956.

Sayah, A, Habelhames, F, Bahloul, A, Nessark, B, Bonnassieux, Y, Tendelier, D & El Jouad, M 2018, 'Electrochemical synthesis of polyaniline-exfoliated graphene composite films and their capacitance properties', Journal of Electroanalytical Chemistry, vol. 818(April 2017), pp. 26–34.

Sayyad, AS, Balakrishnan, K & Ajayan, PM 2011, 'Chemical reaction mediated self-assembly of PTCDA into nanofibers', Nanoscale, vol. 3, no. 9, pp. 3605–3608.

Seidl, L, Bucher, N, Chu, E, Hartung, S, Martens, S, Schneider, O & Stimming, U 2017, 'Intercalation of solvated Na-ions into graphite', Energy and Environmental Science, vol. 10, no. 7, pp. 1631–1642.

Siburian, R, Sihotang, H, Lumban Raja, S, Supeno, M & Simanjuntak, C 2018, 'New route to synthesize of graphene nano sheets', Oriental Journal of Chemistry, vol. 34, no. 1, pp. 182–187.

Sukumaran, SS, Tripathi, S, Resmi, AN, Gopchandran, KG & Jinesh, KB 2019, 'Influence of surfactants on the electronic properties of liquid-phase exfoliated graphene', Materials Science and Engineering B: Solid-State Materials for Advanced Technology, vol. 240(January), pp. 62–68.

Teng, TP, Chang, SC, Chen, ZY, Huang, CK, Tseng, SF & Yang, CR 2019, 'High-yield production of graphene flakes using a novel electrochemical/mechanical hybrid exfoliation', International Journal of Advanced Manufacturing Technology, vol. 104, no. 5–8, pp. 2751–2760.

Uran, S, Alhani, A & Silva, C 2017, 'Study of ultraviolet-visible light absorbance of exfoliated graphite forms', AIP Advances, vol. 7, no. 3.

Gomez, CV, Guevara, M, Tene, T, Villamagua, L, Usca, GT, Maldonado, F, Tapia, C, Cataldo, A, Belluci, S & Caputi, LS 2021, 'The liquid exfoliation of graphene in polar solvents', Applied Surface Science, vol. 546(January), p. 149046.

Vasanthi, V, Logu, T, Ramakrishnan, V, Anitha, K & Sthuraman, K 2020, 'Study of electrical conductivity and photoelectric response of liquid phase exfoliated graphene thin film prepared via spray pyrolysis route', Carbon Letters, vol. 30, no. 4, pp. 417–423.

Wang, M, Xiao, FN, Wang, K, Wang, FB & Xia, XH 2013, 'Electric field driven protonation/deprotonation of 3,4,9,10-perylene tetracarboxylic acid immobilized on graphene sheets via π-π Stacking', Journal of Electroanalytical Chemistry, vol. 688, pp. 304–307.

Wang, S, Wang, C & Ji, X 2017, 'Towards understanding the salt-intercalation exfoliation of graphite into graphene', RSC Advances, vol. 7, no. 82, pp. 52252–52260.

Wang, YZ, Chen, T, Gao, XF, Liu, HH & Zhang, XX 2017, 'Liquid phase exfoliation of graphite into few-layer graphene by sonication and microfluidization', Materials Express, vol. 7, no. 6, pp. 491–499.

Xu, J, Dang, DK, Tran, VT, Liu, X, Chung, JS, Hur, SH, Choi, WM, Kim, EJ & Kohl, PA 2014, 'Liquid-phase exfoliation of graphene in organic solvents with addition of naphthalene', Journal of Colloid and Interface Science, vol. 418, pp. 37–42.

Yang, Q, Zhou, M, Yang, M, Zhang, Z, Yu, J, Zhang, Y, Cheng, W & Li, X 2020, 'High-yield production of few-layer graphene via new-fashioned strategy combining resonance ball milling and hydrothermal exfoliation', Nanomaterials, vol. 10, no. 4, pp. 13–16.

Yassin, AY, Mohamed, AR, Abdelrazek, EM, Morsi, MA & Abdelghany, AM 2019, 'Structural investigation and enhancement of optical, electrical and thermal properties of poly (vinyl chloride-co-vinyl acetate-co-2-hydroxypropyl acrylate)/graphene oxide nanocomposites', Journal of Materials Research and Technology, vol. 8, no. 1, pp. 1111–1120.

Zhang, N, Wang, Z, Song, R, Wang, Q, Chen, H, Zhang, B, Lv, H, Wu, Z & He, D 2019, 'Flexible and transparent graphene/silver-nanowires composite film for high electromagnetic interference shielding effectiveness', Science Bulletin, vol. 64, no. 8, pp. 540–546.

Zhang, Y, Xia, X, Liu, B, Deng, S, Xie, D, Liu, Q, Wang, Y, Wu, J, Wang, X & Tu, J 2019, 'Multiscale Graphene-Based Materials for Applications in Sodium Ion Batteries', Advanced Energy Materials, vol. 9, no. 8, pp. 1–35.

Zhao, X, Zhang, Q & Chen, D 2010, 'Enhanced mechanical properties of graphene-based polyvinyl alcohol composites', Macromolecules, vol. 43, no. 5, pp. 2357–2363.

Zheng, Z & Wang, H 2019, 'Different elements doped graphene sensor for CO2 greenhouse gases detection: The DFT study', Chemical Physics Letters, vol. 721(January), pp. 33–37.